PROCEEDINGS, 48th Workshop on Geothermal Reservoir Engineering
Stanford University, Stanford, California, February 6-8, 2023
SGP-TR-224

Comparison and Analysis of Multiple Scenarios for Enhanced Geothermal Systems Designing Hydraulic Fracturing

Jerjes Porlles [(1)], Olusegun Stanley Tomomewo[(1)], Moones Alamooti[(1,2)], Etochukwu Uzuegbu[(1)]

Institute of Energy Studies, University of North Dakota, Grand Forks 58202, USA (1)
Harold Hamm School of Geology & Geological Engineering, University of North Dakota, Grand Forks 58202, USA (2)

j.porllleshurtado@und.edu, olusegun.tomomewo@und.edu, e.uzuegbu@und.edu moones.alamooti@und.edu.

Keywords: Hydraulic fracturing, geothermal, enhanced geothermal system, simulation.

ABSTRACT

The Enhanced Geothermal Systems (EGS) has been identified as one of the Energy Systems that can support the effort in moving towards net zero if adequately studied and applied. The EGS produces electricity from low permeability rocks and hot dry rocks geothermal resources. Generally, those reservoirs are usually located at 9000ft to 18000ft and temperatures above 160 °C. Principally, the energy is extracted to generate electricity using energy and enhanced energy tools after considering the identified wells environmental, economic, and energetic life cycle. The circulating fluid extracts the geothermal energy between the two wells through fractures. Those fractures are created through hydraulic fracturing treatment. Hence, hydraulic fracturing is the critical technology in the enhanced geothermal system that helps capture the geothermal energy. The potential resource size is vast, and the technology produces baseload, emission-free electricity in line with the net-zero aspirations. Currently, EGS is typically performed in a nearly vertical well, in some cases, water as a heat-transporting fluid. The EGS community is focused on shear stimulation (Gischig, 2015), injecting water to induce slip-on self-propping natural fractures. As a result, proppant is viewed as unnecessary or ineffective; also, the use of packers to enable multiple stages is considered technically infeasible because EGS wells are completed open-hole to maximize connectivity to natural fractures, and reliable open-hole packers are not available at high temperatures. However, in the past several years, the oil and gas industry has achieved radical improvements in stimulation performance by using multiple stages, proppant, and horizontal (or deviated) wells. For the most part, these technologies have not been adopted by EGS.

This study designs a hydraulic fracturing model considering the creation of new fracture sets rather than stimulating natural fractures, comparing a granitoid rock (FORGE) and a very low permeability sedimentary rock. It uses a horizontal injector well completed with cemented casing. Cased hole packers or bridge plugs are used for zonal isolation, allowing multiple-stage fracture treatments to be pumped through perforations in the casing. This research aims to study the feasibility of creating permeable cracks by hydraulic fracturing and evaluating geomechanical properties such as young's modulus and Poisson's ratio in a bit to produce energy. Hence, the result of this study shows that an EGS design with multiple stages and improved geomechanical properties increase economic performance relative to current procedures.

1. INTRODUCTION

We implemented an analysis to evaluate the feasibility of developing an enhanced geothermal system (EGS) project, considering the evaluation and design of a horizontal well stimulated by hydraulic fracturing, including fracture fluids and types of proppants that could be used in a frac job (Liang, 2016). The evaluation covers a conceptual representation of a granitoid reservoir and a very-low sedimentary reservoir.

The rock composition of those reservoirs impacts the rock's geomechanical properties, petrographically (mineral composition) and texturally (grain size, shape, and sorting). It is imperative to have in-depth insight into how they impact Young's modulus, hardness, brittleness, and Poisson's ratio (Brotons, 2016). Many shale strata will react differently to hydraulic fracturing due to differences in makeup and texture (Passey, 2010). Knowing the factors influencing shale's geomechanical properties is crucial for optimizing the formation response to hydraulic fracture stimulation (Ttian, 2017). Hydraulic fracking procedures are evaluated using two geomechanical parameters; Poisson's ratio and Young's modulus (Rickman, 2008; Labani and Rezaee, 2015). In practice, rocks with a high Young's modulus and a low Poisson's ratio are considered brittle, meaning they are much more prone to fracture under stress and retain open fractures. The opposite is true for rocks with a lower Young's modulus and a higher Poisson's ratio; these rocks are more resistant to fracture initiation because of their ductility (Rickman et al., 2008). The mineral content of rocks (such as clay, feldspar quartz, pyrite, and carbonate) and total organic carbon (Aoudia, 2010 and Harris, 2011) have been attributed to these characteristics in certain research. Carbonate and quartz are brittle minerals, while organic matter and clay are ductile (Sondergeld, 2010).

The brittleness index is the percentage of brittle minerals relative to the total number of minerals in shale, as stated by Jarvie (2007). By their criteria, brittleness index = quartz/ (quartz + carbonate + clay) (Keikha, 2013). Based on their assumptions, quartz is the sole brittle

mineral. Dolomite was identified by Wang and Gale (2009) as a significant contributor to shale brittleness, hence redefining to brittleness index = (quartz + dolomite)/ (quartz + dolomite + limestone + clay + total organic carbon). Meng (2021) mentions the application of rock brittleness indices and their applications to different fields.

Figure 1 shows the relationship between Young's modulus, Poisson's ratio, ductility, and brittleness of some rocks from two well in Maxhamish and Imperial Komie, Canada.

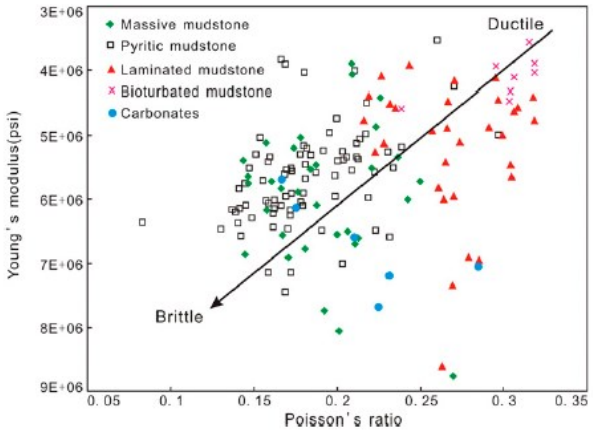

Figure 1. Cross plot of young's modulus versus Poisson's ratio of samples from different lithofacies for EOG Maxhamish D-012-L/094-15O and Imperial Komie D-069-K/094-O-02 wells (Tian Dong et al.,2016).

The granite's geological makeup (mineral type and grain size) determines the rock's mechanical characteristics. It would be helpful in engineering and building if these mechanical qualities could be predicted using mineralogical factors. Grain sizes (average and per mineral), mineral composition (quartz, alkali feldspar, plagioclase, and micas), density, and Mohs hardness were some of the geological characteristics of rocks that could be used to evaluation of the following mechanical qualities: Unconfined Compressive Strength (UCS), crack initiation stress (CI), crack damage stress (CD), Young's Modulus (E), Poisson's ratio (v). Cowie and Walton (2018) utilized the average grain size and standard deviation of grain sizes of the minerals, as well as the minimum, maximum, average, and typical variation of the entire sample grain size, to demonstrate the relationship. As with plutonic rocks, the granitic rocks were classified according to their mineralogical constituents using Streckeisen's classification scheme (Streckeisen, 1976). Figure 2 shows a classification based on the percentage composition of three critical minerals, Quartz, Alkali Feldspar, and Plagioclase Feldspar (Tuğrul, 1999). Applying this scheme, different granitic rocks were classified using mineral type and gran size by the right of the figure and where each plot in the figure was.

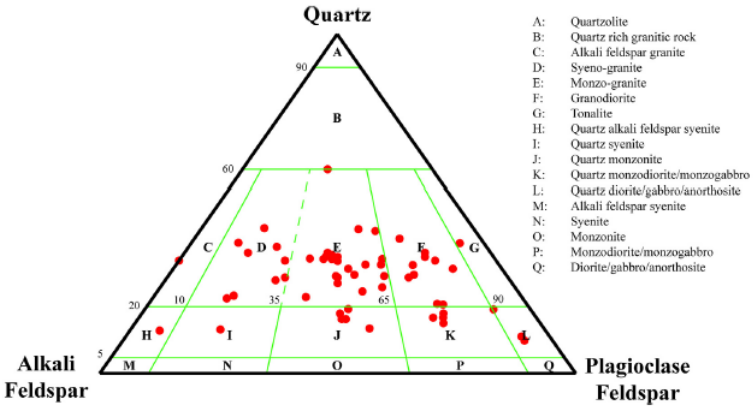

Figure 2. Classification of granites based on the plot of coarse grain size and mineralogy (Streckeisen, 1976).

Mishra (2017) explains that quartzite and dolomite are brittle rocks with an elastic-failure behavior; however, granite has a plastic-elastic behavior. Figure 3 shows the stress-strain (σ - ε) curve for granite, sandstone, and dolomite behavior.

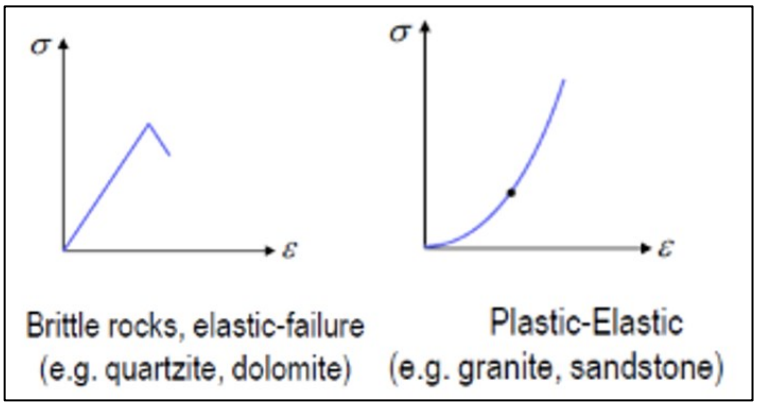

Figure 3. Stress – strain (σ - ε) curve for granite, sandstone, and dolomite behavior (Rasouli, 2017).

Stimulation by hydraulic fracturing in EGS has been developed around the world. According to Moska et al. (2021), these projects were designed, for the most part, on granite rocks characterized by low porosity and permeability, located at a depth of 2.7–5.5 km, and temperatures between 150 to 300 ◦C. Regarding hydraulic fracturing simulation models on EGS, McClure et al. (2022) presented a study related to modeling a multistage hydraulic stimulation; this paper explains that a massive HF can potentially trigger more EGS jobs. Geothermal stimulation is currently designed for a single-stage, which is not economical to develop an EGS project. Nowadays, the EGS projects have been developed and improved to face a new frontier in the geothermal industry. Utah-Forge is developing an EGS project, drilling through a granitoid formation (Nadimi et al., 2018); this EGS thermal reservoir has been stimulated to produce heat from a very low permeability reservoir. Another critical project under execution is the DEEP Geothermal Power Project, located in Southeastern Saskatchewan, Canada. DEEP drilled a wildcat well in 2018 (3.55 km), and well tests showed bottom-hole temperatures higher than 125˚C (Groenewoud & Marcia, 2020). Also, Altarock Energy is developing an EGS project in Oregon, USA. The project aims to test the feasibility of producing energy, creating permeable cracks by hydraulic fracturing (Bonneville et al., 2018). However, these projects developed an HF in vertical or deviated wells. According to Moska et al. (2021), some EGS experimental projects have used slickwater to avoid high-power fracturing equipment at low pumping rates. Also, Lei (2019) develops a fracture model using slickwater under different conditions. McClure (2014) analyzed the mechanisms of stimulation in various EGS projects. He points out that flow is from preexisting fractures during injection, bottom-hole pressure is more than the minimum principal stress, and some pressure limitations exist. Li et al. (2015) developed an analysis of hydraulic fracturing and the reservoir behavior in EGS, considering the fluid flow's impact through the reservoir, the distance between fracture, petrophysical properties, and several fractures were evaluated, recommending fracture length (Lecampion, 2013).

Lab studies related to EGS were developed. Li (2015) presented experimental research on HF in EGS through a high-temperature true-triaxial hydraulic fracturing test system. This study is critical because most studies of hydraulic fracturing have been done for sandstone and limestone in the oil and gas industry; this study provides geomechanical properties to design a hydraulic fracturing in a granite rock. The author explains that parameters such as initiation and propagation of HF for sandstone and limestone can be simulated in the true-triaxial hydraulic fracturing test system; nonetheless, EGS reservoirs have some differences due to the rock lithology, and high temperature has to be reached. This model explains the matrix deformation, how HF causes deformation, and whether the hot rock with natural fractures will benefit the geothermal project (Watanabe, 2017). Geothermal reservoir exploration relies heavily on reservoir quality, highlighting petrophysics' significance. The theory and methodology are similar to petrophysics used in petroleum exploration and production, although the emphasis is on a different set of problems. Lithology, porosity, permeability, and water saturation of the drilled section are all part of the interpretation process.

Cuttings, cores, and side-wall cores can be used to determine reservoir parameters and obtain detailed lithological information precisely. Reservoir parameters, however, cannot be determined from cuttings, and the number and duration of cored intervals are typically limited. Therefore, determining lithology and reservoir characteristics in most wells requires deciphering the information in various petrophysical well logs. Gamma-ray (GR) logs, neutron (NPHI) logs, and density (RHOB) logs are the primary logs used for determining lithology. Sandstone and limestone effective porosity (PHIE) can be understood using GR, NPHI, and RHOB logs. Combining log interpretation with core analysis, petrography, and diagenesis data of reservoir sections may optimize reservoir quality prediction. Combining PHIE with core analysis data (porosity and permeability) allows for creating a synthetic permeability log, which may be used as a reliable model of reservoir performance. The transmissivity of reservoir sections can be calculated for use in geothermal studies. This section of the paper summarizes the review study, comparing the petrophysical and geomechanical properties of the different rock types, including sedimentary and igneous rocks (Li, 2020).

Table 1: Petrophysical and geomechanical properties of typical rocks (Pratt, 1972, Xing, 2021, Josh, 2012)

Rock Type	Permeability (μD)	Porosity	Thermal Conductivity (Wm−1 K−1)	Volumetric Rock type Thermal Expansion (10^{-5} ºC)	Specific heat (10^3 J/kg K)	Geothermal Gradient (°C km^{-1})	Density (kg/m)	E (Gpa)	Poisson's Ratio
Granite	0.5 – 2.0	0.01	2.92	2.4	1.07	35.3	2530	30-70	0.25
Shale	10 - 20	0.05	1.64	3.4	0.8	51	2200	45076	0.1

2. FRACTURE PROPAGATION DESIGN

Underground rock stress is evaluated to model how hydraulic fracturing increases the surface area of the wellbore to connect with the reservoir by high-pressure fluid. Hydraulic fracturing modeling implies three processes. First, the rock induced mechanical deformation due to fluid pressure at the fracture surface, fluid flow through the fracture, and fracture propagation. Rock deformation is modeled using linear elastic theory, represented by an equation determining a relationship between fluid and fracture width pressure. Also, fluid flow is represented by the partial differential equation that connects fluid flow velocity, fracture width, and gradient fracture. Finally, fracture propagation is represented by the flow of energy liberation, and 2D and 3D models can be developed. To develop a 2D hydraulic fracture model, Khristianovich-Geertsma, De Klerk (KGD), Perkins-Kern-Nordgren (PKN), and the radial model can be used (Calderon, 2013; Porlles, 2022); however, to develop a 3D model, hydraulic fracture simulators have been used.

2.1. KGD hydraulic fracture Modeling

KGD is a 2D hydraulic fracturing model and has some assumptions. The formation is an infinite, homogeneous, isotropic, linear elastic medium characterized by young's modulus, Poisson's ratio, and toughness. Fracture is assumed to be radially symmetric and generated from a point source at its center. The periphery of the fracture is circular. A viscous Newtonian fracturing fluid is injected with a constant volumetric flow rate and laminar flow. Finally, gravitational effects are not considered (Calderon, 2013).

$$L = 0.48 \left[\frac{8G_{dyn}Q^3}{(1-\upsilon)\mu}\right]^{1/6} (t)^{2/3} \quad (1)$$

$$Wo = 1.32 \left[\frac{8(1-\nu)\mu Q^3}{G_{dyn}}\right]^{1/6} (t)^{1/3} \quad (2)$$

$$P_w = S_h + 0.96 \left[\frac{2Q\mu {G_{dyn}}^3}{(1-\upsilon)L^2}\right]^{1/4} \quad (3)$$

$$P_w - P = \frac{12Q\mu L}{h_f}\int_{f_{L_w}}^{f_L} \frac{d\,f_L}{w^3} \quad (4)$$

Where L is fracture length, G_{dyn} is the shear modulus, Q is the fracture flow rate, μ is the viscosity fracture fluid, t is the fracture time, Wo is the fracture width, P_w is the fracture pressure, h_f is the fracture height, f_L is x/L relationship, x is the propagation length, f_{L_w} is the relationship between wellbore radius and fracture length, and r_w is the wellbore radius.

2.2 PKN hydraulic fracture Modeling

This model uses an analytical solution to model the geometry of a hydraulic fracture. The thickness of the fracture varies both in the vertical section and along the fracture length. This geometry is considered if the length of the fracture is considerably more than its height.

$$L = 0.68 \left[\frac{G_{dyn}Q^3}{(1-\upsilon)\mu \square_f{}^4}\right]^{1/5} (t)^{4/5} \quad (5)$$

$$Wo = 2.5 \left[\frac{(1-\nu)\mu Q^2}{G_{dyn}h_f}\right]^{1/5} (t)^{1/5} \quad (6)$$

$$P_w = 2.5\left[\frac{Q^2\mu {G_{dyn}}^4}{(1-v)^4 {h_f}^6}\right]^{1/5}(t)^{1/5} \quad (7)$$

$$\frac{d\,P}{d\,x} = -\frac{64Q\mu}{\pi h_f w^3} \quad (8)$$

2.3 Radial Model

This model assumes that the fluid pressure remains constant. This model is applicable in homogeneous reservoirs when there are no barriers that limit the growth in the height of the fracture or when a horizontal fracture is created, and when the distribution of the minimum stress is uniform.

$$R = 0.548\left[\frac{G_{dyn}Q^3}{\mu}\right]^{1/9}(t)^{4/9} \quad (9)$$

$$Wo = 21\left[\frac{\mu^2 Q^3}{{G_{dyn}}^2}\right]^{1/9}(t)^{1/9} \quad (10)$$

$$P_w = \sigma_{min} - \frac{5}{4\pi}\frac{GWo}{R}\,Ln\frac{r_w}{R} \quad (11)$$

$$P_w - P = \frac{6Q\mu}{\pi}\int_{f_{rw}}^{f_r}\frac{d\,f_r}{w^3} \quad (12)$$

In the oil & gas industry, the height of the fracture usually is the thickness of the reservoir. Nonetheless, EGS reservoirs (granite) have a longer thickness; we can assume no top and bottom boundaries. A radial symmetric fracture is more suitable for simulating an EGS reservoir. According to the description of the three models, the radial model fits better to design hydraulic fracturing for a granite reservoir because granite has geomechanical and petrophysical homogeneous properties.

3. MASS FLOW RATE AND THERMAL ENERGY RECOVERABLE

The mass flow and heat recoverable were evaluated for each combination of parameters (fracture length, fracture width, fracture permeability, number of stages), modeling the geometry of a vertical and horizontal section of a typical well similar to the Bakken formation. The bottom hole pressure of the injector was set at a pressure lower than the fracture pressure of 75 MPa. A thermal simulator was used to develop a mathematical model where Darcy's law equation is applied to design the velocity of a fluid phase; this model describes the interactions between permeability, saturation, viscosity, and pressure difference. The thermal model considers the water phase (w) and steam phase (s) in our case (McClure, 2022; Aliyu, 2017).

$$u_w = \frac{\bar{K}k_{rw}}{\mu_w}\left(\frac{\partial P_w}{\partial x_j} - \rho_w\bar{g}\right) \quad (13)$$

$$u_s = \frac{\bar{K}k_{rs}}{\mu_s}\left(\frac{\partial P_s}{\partial x_j} - \rho_s\bar{g}\right) \quad (14)$$

Where u is the velocity of phase, μ is the viscosity of phase, P is the pressure, $\bar{K}$ is the permeability, and $\bar{g}$ is the gravitational acceleration. The mass balance of water and steam is defined as:

$$-\frac{\partial(u_w\rho_w)}{\partial x_i} + q_w - d_v = \frac{\partial(\phi S_w\rho_w)}{\partial t} \quad (15)$$

$$-\frac{\partial(u_s\rho_s)}{\partial x_i} + q_s + d_v = \frac{\partial(\phi S_s\rho_s)}{\partial t} \quad (16)$$

Where ρ is the average density, q is the volumetric flow rate, d_v is the vaporization rate, Sw is the water saturation, and Ss is the vapor saturation. Equations are reorganized, and the flow rate is described in the porous medium, considering a pressure difference between the two phases. This pressure difference is defined as capillary pressure $P_c = P_s + P_w$.

$$\frac{\partial\left\{\frac{\bar{K}k_{rw}\rho_w}{\mu_w}\left(\frac{\partial P_w}{\partial x_j} - \rho_w\bar{g}\right)\right\}}{\partial x_i} + q_w - d_v = \frac{\partial(\phi S_w\rho_w)}{\partial t} \tag{17}$$

$$\frac{\partial\left\{\frac{\bar{K}k_{rs}\rho_s}{\mu_s}\left(\frac{\partial P_s}{\partial x_j} - \rho_s\bar{g}\right)\right\}}{\partial x_i} + q_s + d_v = \frac{\partial(\phi S_s\rho_s)}{\partial t} \tag{18}$$

Equation 18 shows the energy balance of water, steam, and rock, assuming that movement of steam and water through the reservoir is adequately slow, the surface area of water and steam are amply large, the thermal equilibrium exists between water, steam, and rock (Mercer et al., n.d.-a). Hence, considering these assumptions, it is possible to describe the energy-balance equation:

$$-\frac{\partial(u_w\rho_w H_w + u_s\rho_s H_s)}{\partial x_i} + q_w H_w + q_s H_s + \frac{\partial(\bar{\bar{K}}_m\frac{\partial T}{\partial x_j})}{\partial x_i} = \frac{\partial(\phi\rho H + (1-\phi)H_r\rho_r)}{\partial t} - \frac{\partial\phi p}{\partial t} + (u_w + u_s)\frac{\partial p}{\partial x_i} \tag{19}$$

Where H_s is the enthalpy of saturated steam, H_w is the enthalpy of saturated water, T is the reservoir temperature, $\bar{\bar{K}}_m$ is the thermal dispersion tensor for the medium, ρ_r is the average rock density, h_r is the rock enthalpy, and H is the total enthalpy of the mixture. It is defined as H= (Ss ρsHs+ Ss ρsHs)/ρ.

4. MODELING FLOW RATE

The mass flow rate is evaluated to determine the recoverable energy. The recoverable energy (j) in a period is defined as (McClure, 2022, Deo, 2014):

$$Q_{rec} = \dot{q}c_w(\Delta T_j)\ (\Delta t_j) \tag{20}$$

Where c_w is the heat capacity of the fluid produced, $\dot{q}$ is the mass flow rate, Δt_j is the period of the project (30 years), and ΔT_j is the difference between production temperature and the power plant outlet temperature (Li, 2015).

The thermal energy to generate electricity is calculated with the following equation:

$$E_j = Q_{rec}eff \tag{21}$$

Where eff is the net cycle thermal efficiency, this project uses a net cycle thermal efficiency of 10 %.

5. RESULTS AND DISCUSSION

5.1 Fracture propagation design

According to the different analytical 2D models (PKN, KGB, and Radial), we evaluate fracture length and fracture width at different Poisson's ratios. Considering FORGE (granitoid), the range of 0.26 to 0.3 Poison's ratio and the range for low permeability sedimentary rock is 0.1 to 0.35 (Xing, 2021). For the FORGE reservoir, the fracture length ranges from 260 to 280 m, and a fracture width between 22 to 25 mm. (Figure 4). Concerning low permeability sedimentary rock. Figure 4 shows the results for the low permeability sedimentary; the fracture length ranges from 220 to 250 m, and a fracture width between 25 to 30 mm. (Figure 5).

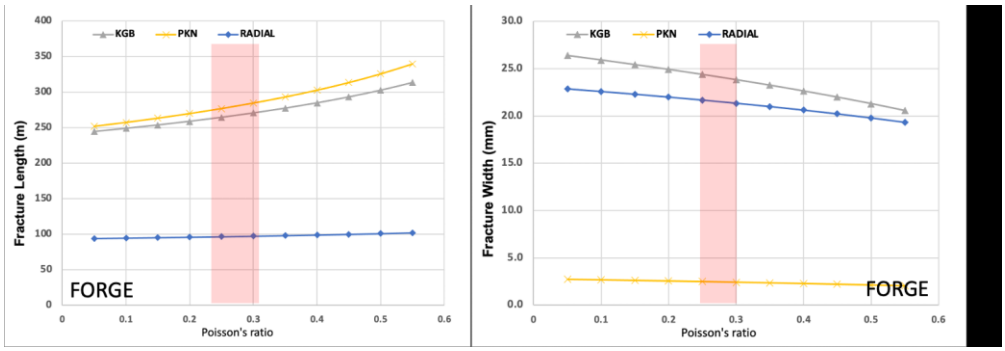

Figure 4. Fracture length and width vs. Poisson's ratio (FORGE)

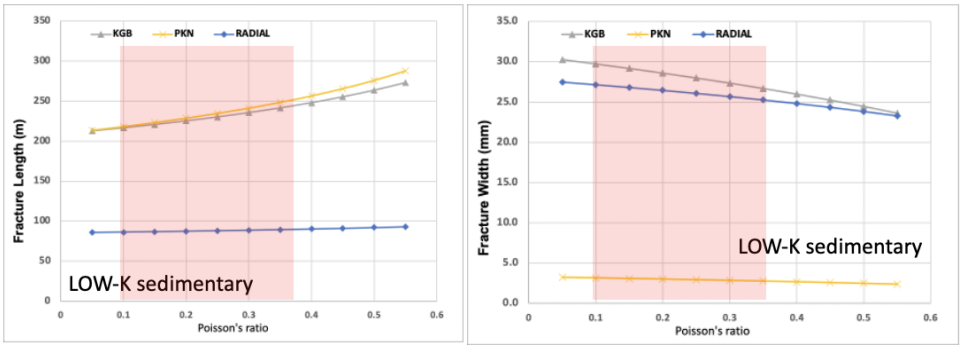

Figure 5. Fracture length and width vs. Poisson's ratio (Low-K sedimentary)

In addition to the 2D model, we developed a 3D model using a numerical simulator which combine hydraulic fracturing simulation and reservoir modeling. Figure 6 compares the fracture length of FORGE (granitoid) and low permeability sedimentary rock. We can see that granitoid generate more fracture propagation compared to the low permeability sedimentary rock.

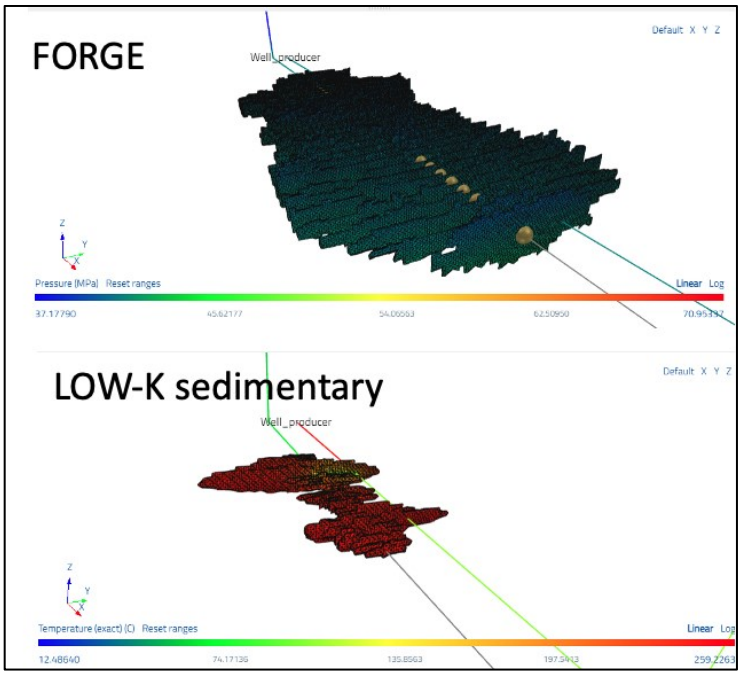

Figure 6. Fracture length (FORGE vs. Low K sedimentary)

Figure 7 compares FORGE (granitoid) fracture length and low permeability sedimentary rock. We can see that fracture propagation of the granitoid rock is higher than the low permeability sedimentary rock. On the contrary, Figure 7 shows that the fracture width of the granitoid rock is lower than the low-permeability sedimentary rock.

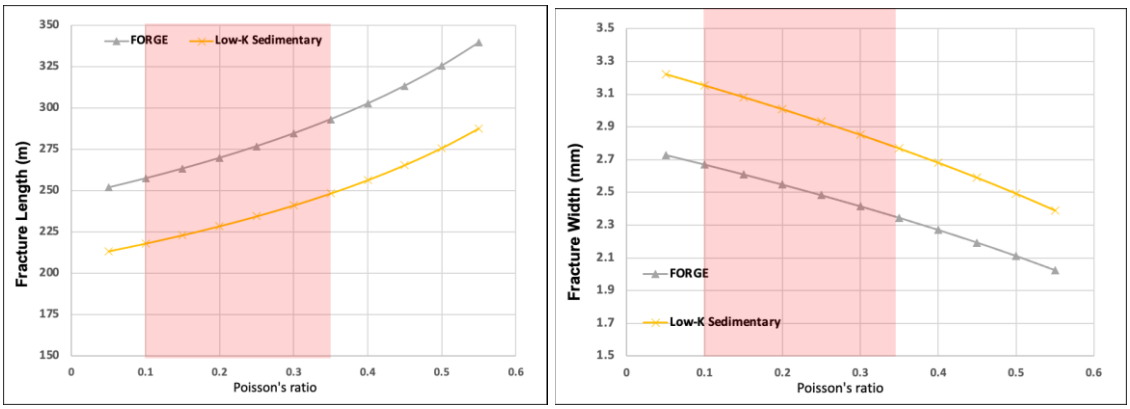

Figure 7. Fracture length and fracture width (FORGE vs Low K sedimentary)

5.2 Determination of Recoverable Energy

A numerical simulation made different runs to determine the recoverable energy of a granitoid and the low permeability sedimentary reservoir and the fracture propagation designing horizontal wells stimulated by hydraulic fracturing. The reservoir (Utah-Forge) has very low porosity and permeability. The reservoir model is designed with 50 grids of 50 meters in the y-direction and 70 grids of 50 meters in the x-direction. Although we consider a reservoir thickness of 500m, the real reservoir thickness is not determined, and the temperature log determines the reservoir temperature. In contrast, low permeability sedimentary has clear limits. We developed two different case studies to acquire data (Franco, 2017). The first case is a pattern of two horizontal wells (one production well/one injection well). Table 2 shows the total initial energy in place using reservoir properties included in Table 1, in which total initial energy in situ was calculated volumetrically. Also, the abandoned temperature considerate will be 50°C.

Table 2. Initial Energy in situ

Description	FORGE	Low-K sedimentary	units
Area	8.75	8.75	km2
Reservoir Thickness	500	200	m
Rock density	2530	2200	Kg/m3
Water density	997	997	Kg/m3
Reservoir temperature	210	210	°C
Initial energy in the rock	1.511E+18	1.241E+18	J
Initial energy in reservoir fluids	0.017E+18	0.014E+18	J
Total Initial energy in place	1.529E+18	1.255E+18	J

Figure 8 shows the accumulated energy for both cases. The Forge project accumulated 2.3 E+09 MJ, and the low-permeability sedimentary 1.7E+09 MJ, respectively. Finally, Figure 9 shows the electricity generation rate was evaluated; the Forge project generated 0.22 MWe, and the low-permeability sedimentary was 0.17 MWe, respectively, considering a factor plant of 0.1.

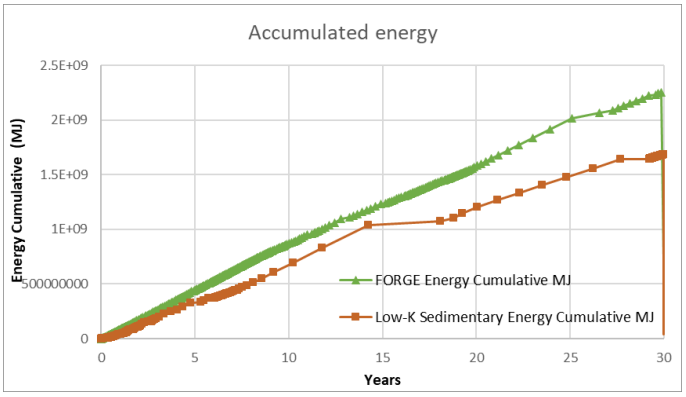

Figure 8. Accumulated energy (MJ)

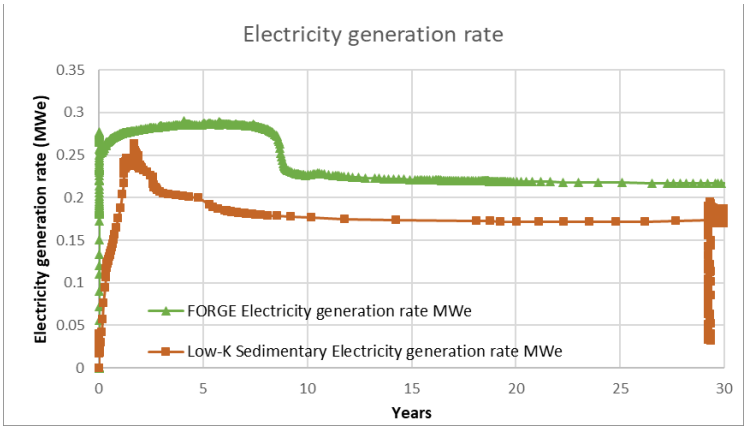

Figure 9. Summary of electricity generation rate

4. CONCLUSIONS

- Enhanced Geothermal Systems have a huge potential due to the advantages such as producing baseload, emission-free electricity in line with the net-zero emissions aspirations. Although EGS technology is focused on shear stimulation, injecting water to induce slip-on self-propping natural fractures and proppant is viewed as unnecessary or ineffective; hydraulic fracturing would be a better option to use due to, in the last decade, the oil and gas industry has achieved radical improvements in stimulation performance by using multiple stages, proppant, and horizontal (or deviated) wells. For the most part, these technologies have not been adopted by EGS.

- This study evaluated a hydraulic fracturing model considering the creation of new fracture sets, comparing a granitoid rock (FORGE) and a very low permeability sedimentary rock. So, this study designed a horizontal injector well completed with cemented casing and a horizontal production well with open hole completion. This research aimed to study the feasibility of producing energy, creating permeable cracks by hydraulic fracturing, and evaluating geomechanical properties such as young's modulus and Poisson's ratio. Hence, this study has shown that an EGS design with multiple stages and proppant can improve economic performance relative to current procedures.

- This study showed the feasibility of applying a hydraulic fracturing treatment in an EGS reservoir in a granitoid and a very low permeability sedimentary rock. Petrophysics and geomechanical properties were used from the Utah-FORGE project and sedimentary rock to generate 2D and 3D hydraulic fracturing models. Although there is no hydraulic fracturing in horizontal wells for EGS purposes due to the barrier of the high initial investment, the current price of electricity can promote this type of project.

- This study shows that the rock composition of granitoid and low permeability sedimentary rock impacts the rock's geomechanical properties. Rocks with a high Young's modulus and a low Poisson's ratio are considered brittle, meaning they are much more prone to fracture under stress and retain open fractures. Our results show that rocks with high Young modulus have more fracture propagation (granitoid). However, rocks with a lower Young's modulus and a higher Poisson's ratio are more resistant to fracture initiation because of their ductility.

- According to the description of the three 2D models, the PKN and KGB models fit better to design hydraulic fracturing. EGS reservoirs (granitoid) have a longer thickness; we assumed top and bottom boundaries. Nonetheless, the 3D model developed in the simulator and previous EGS jobs matches with a KGD model where the fracture length has shown to be 260m on average, with a maximum fracture length of 350m. Additionally, fracture height averages 63m and a maximum fracture height of 76m.

- We evaluated different 2D models (PKN, KGB, and Radial) of fracture length and width at different Poisson ratios. Considering FORGE (granitoid), the range of 0.26 to 0.3 Poison's ratio and the range for low permeability sedimentary rock is 0.1 to 0.35. For the FORGE reservoir, the fracture length ranges from 260 to 280 m, and a fracture width between 22 to 25 mm. (Figure 3). Concerning low permeability sedimentary rock. The results for the low permeability sedimentary; the fracture length ranges from 220 to 250 m, and a fracture width between 25 to 30 mm.

- We developed a 3D model to compare FORGE (granitoid) fracture length and low permeability sedimentary rock. Fracture propagation of the granitoid rock is higher than the low permeability sedimentary rock. On the contrary, the fracture width of the granitoid rock is lower than the low-permeability sedimentary rock.

- The Forge project accumulated 2.3 E+09 MJ, and the low-permeability sedimentary 1.7E+09 MJ, respectively. Finally, the electricity generation rate was evaluated; the Forge project generated 0.22 MWe, and the low-permeability sedimentary was 0.17 MWe, respectively, considering a factor plant of 0.1.

REFERENCES

Aliyu, M., Chen, H.-P., Aliyu, M. D., Harireche, O., & Hills, C. D. (2017). Numerical Modelling of Geothermal Reservoirs with Multiple Pore Media. https://www.researchgate.net/publication/327968207

Aoudia, K., J. L. Miskimins, N. B. Harris, and C. A. Mnich, 2010, Statistical analysis of the effects of mineralogy on rock mechanical properties of the Woodford shale and the associated impacts for hydraulic fracture treatment design: 44th US Rock Mechanics Symposium and 5th US–Canada Rock Mechanics Symposium, Salt Lake City, Utah, June 27–30, 2010, 11 p.

Brotons, V., Tomás, R., Ivorra, S., Grediaga, A., Martínez-Martínez, J., Benavente, D., & Gómez-Heras, M. (2016). Improved correlation between the static and dynamic elastic modulus of different types of rocks. Materials and Structures/Materiaux et Constructions, 49(8), 3021–3037. https://doi.org/10.1617/s11527-015-0702-7

Calderon, C. Z. (2013). Introducción a la Mecánica de Rocas. Universidad Industrial de Santander, Facultad de Ingenierías Fisico-químicas, Escuela de Ingeniería en Petróleos.

Cowie S and Walton G (2018), The effect of mineralogical parameters on the mechanical properties of granitic rocks. https://doi.org/10.1016/j.enggeo.2018.04.021

Deo, M., Roehner, R., Allis, R., & Moore, J. (2014). Modeling of geothermal energy production from stratigraphic reservoirs in the Great Basin. Geothermics, 51,

Franco, A., & Donatini, F. (2017). Methods for the estimation of the energy stored in geothermal reservoirs. Journal of Physics: Conference Series, 796(1). https://doi.org/10.1088/1742-6596/796/1/012025

Gischig, V. S., & Preisig, G. (2015). Hydro-fracturing versus hydro-shearing: A critical assessment of two distinct reservoir stimulation mechanisms. 13th ISRM International Congress of Rock Mechanics, 2015-MAY, 1–12. https://doi.org/10.13140/RG.2.1.4924.3041

Jarvie, D. M., R. J. Hill, T. E. Ruble, and R. M. Pollastro, 2007, Unconventional shale-gas systems: The Mississippian Barnett Shale of north-central Texas as one model for thermogenic shale-gas assessment: AAPG Bulletin, v. 91, no. 4, p. 475–499, doi:10.1306/12190606068.

Josh, M, Esteban, L. (2012). Laboratory characterization of shale properties. Journal of Petroleum Science and Engineering, Volumes 88–89, 2012, Pages 107-124, ISSN 0920-4105, https://doi.org/10.1016/j.petrol.2012.01.023.

Keikha and Keykha, (2013).Correlation between mineralogical characteristics and engineering properties of granitic rocks. January 2013: Electronic Journal of Geotechnical Engineering 18:4055-4065.

Harris, N. B., J. L. Miskimins, and C. A. Mnich, 2011, Mechanical anisotropy in the Woodford shale, Permian Basin: Origin, magnitude, and scale: Leading Edge, v. 30, no. 3, p. 284–291, doi:10.1190/1.3567259.

Lecampion, B., & Desroches, J. (2015, October 13). Geomechanical Drivers of the (in)-Efficiencies of Multi-stage Hydraulic Fracturing. https://doi.org/10.3997/2214-4609.201414291

Li, M., & Lior, N. (2015). Analysis of hydraulic fracturing and reservoir performance in enhanced geothermal systems. Journal of Energy Resources Technology, Transactions of the ASME, 137(4). https://doi.org/10.1115/1.4030111

Li, Y., Zhou, L., Li, D., Zhang, S., Tian, F., Xie, Z., & Liu, B. (2020). Shale brittleness index based on the Energy Evolution Theory and evaluation with logging data: A case study of the guandong block. ACS Omega, 5(22), 13164–13175. https://doi.org/10.1021/acsomega.0c01140

Liang, F., Sayed, M., Al-Muntasheri, G. A., Chang, F. F., & Li, L. (2016). A comprehensive review on proppant technologies. In Petroleum (Vol. 2, Issue 1, pp. 26–39). KeAi Communications Co. https://doi.org/10.1016/j.petlm.2015.11.001

McClure, Mark, Kang, Charles, and Garrett Fowler. (2022) "Optimization and Design of Next-Generation Geothermal Systems Created by Multistage Hydraulic Fracturing." Paper presented at the SPE Hydraulic Fracturing Technology Conference and Exhibition, The Woodlands, Texas, USA, February 2022.

Meng, F., Wong, L. N., & Zhou, H. (2021). Rock brittleness indices and their applications to different fields of Rock Engineering: A Review. Journal of Rock Mechanics and Geotechnical Engineering, 13(1), 221–247. https://doi.org/10.1016/j.jrmge.2020.06.008

Mishra, S., Meena, H., Parashar, V., Khetwal, A., Chakraborty, T., Matsagar, V., Chandel, P., & Singh, M. (2017). High strain rate response of rocks under dynamic loading using split Hopkinson pressure bar. Geotechnical and Geological Engineering, 36(1), 531–549. https://doi.org/10.1007/s10706-017-0345-2

Moska, R., Labus, K., & Kasza, P. (2021). Hydraulic fracturing in enhanced geothermal systems—field, tectonic and rock mechanics conditions—a review. In Energies (Vol. 14, Issue 18). MDPI. https://doi.org/10.3390/en14185725.

Nadimi, S., Forbes, B., Finnila, A., Podgorney, R., Moore, J., & McLennan, J. D. (2018). Hydraulic Fracture/Shear Stimulation in an EGS Reservoir: Utah FORGE Program. In 52nd U.S. Rock Mechanics/Geomechanics Symposium.

Pratt, H. Black, W.(1972). The effect of speciment size on the mechanical properties of unjointed diorite. International Journal of Rock Mechanics and Mining Sciences & Geomechanics Abstracts. Volume 9, Issue 4, 1972, Pages 513-516, ISSN 0148-9062, https://doi.org/10.1016/0148-9062(72)90042-3.

Porlles, J. W., & Jabbari, H. (2022). Simulation-based economical modeling of hydraulic fracturing for Enhanced Geothermal System. All Days. https://doi.org/10.56952/arma-2022-2326

Rickman, R., M. J. Mullen, J. E. Petre, Bill Grieser, and D. Kundert, SPE, Halliburton, 2008, A Practical Use Of Shale Petrophysics for Simulation Desigin Optimization: All Shale Plays Are Not Clones of the Barnet Shale, SPE 115258. https://d1jxr8mzr163g2.cloudfront.net/396eaf6c-77e7-4de3-ab62-b45d4a23b559/a6add290-5e56-4cc4-9ac4-fb59c38c5a5e.pdf

Rasouli, V (2017). Rock Mechanics. Fundamentals. University of North Dakota.

Passey, K. M. Bohacs, W. L. Esch, R. Klimentidis, and S. Sinha, ExxonMobil Upstream Research Co. From Oil-Prone Source Rock to Gas-Producing Shale Reservoir – Geologic and Petrophysical Characterization of Unconventional Shale-Gas Reservoirs : SPE 131350. https://fffcarbon.co.za/articles/2012/SPE-131350-FINAL-Low_Passey-et-al_.pdf

Sondergeld, C. H., K. E. Newsham, M. C. Rice, and C. S. Rai, 2010, Petrophysical considerations in evaluating and producing shale gas resources: SPE Unconventional Gas Conference, Pittsburgh, Pennsylvania, February 23–25, 2010, SPE-131768-MS, 34 p., doi:10.2118/131768-MS.

Streckeisen, A.L. (1976) Classification of the Common Igneous Rocks by Means of Their Chemical Composition: A Provisional Attempt. Neues Jahrbuch fur Mineralogie, Monatshefte, 1, 1-15.

Ttian Dong, Nicholas B Harris, Korhan Ayranci, and Sheng Yang (2017). The impact of rock composition on geomechanical properties of a shale formation: Middle and Upper Devonian Horn River Group shale, Northeast British Columbia, Canada, Article in AAPG Bulletin · February 2017 DOI: 10.1306/07251615199

Tuğrul, A. and Zarif, I.H. (1999) Correlation of Mineralogical and Textural Characteristics with Engineering Properties of Selected Granitic Rocks from Turkey. Engineering Geology, 51, 303-317. https://doi.org/10.1016/S0013-7952(98)00071-4

Wang, F. P., and J. F. W. Gale, 2009, Screening criteria for shale-gas systems: Transactions of the Gulf Coast Association of Geological Societies, v. 59, p. 779–793.

Watanabe, N., Egawa, M., Sakaguchi, K., Ishibashi, T., & Tsuchiya, N. (2017). Hydraulic fracturing and permeability enhancement in granite from subcritical/brittle to supercritical/ductile conditions. Geophysical Research Letters, 44(11), 5468–5475. https://doi.org/10.1002/2017gl073898

Xing. P,Damjanac, B (2021). Numerical Simulation of Injection Tests at Utah FORGE Site. PROCEEDINGS, 46th Workshop on Geothermal Reservoir Engineering Stanford University, Stanford, California, February 16-18, 2021 SGP-TR-218.